

PAPER

[View Article Online](#)
[View Journal](#) | [View Issue](#)

Cite this: *Dalton Trans.*, 2014, **43**, 6643

A rhomboid-shaped organic host molecule with small binding space. Unsymmetrical and symmetrical inclusion of halonium ions†

Yuji Suzaki, Takashi Saito, Tomohito Ide and Kohtaro Osakada*

Received 4th January 2014,

Accepted 5th February 2014

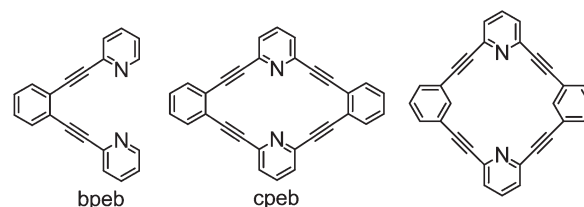
DOI: 10.1039/c3dt53629g

www.rsc.org/dalton

A shape persistent rhomboid-shaped organic host molecule having two pyridyl units was synthesized which induces size selective halonium inclusion. Cl^+ and Br^+ are included to form unsymmetric and symmetric complexes, while I^+ does not form a stable complex. The difference among the haloniums was ascribed to the matching (or mismatching) of the shape of the cavity and the guest ions. The complexation of the host molecule with other cations, such as Ag^+ , Pd^{2+} , Zn^{2+} and H^+ , is also mentioned.

Introduction

Macrocyclic organic host molecules, such as crown ethers,¹ cryptands,² calix arenes,³ pillararenes⁴ and cyclodextrins,⁵ bind guest molecules as well as ions to form inclusion complexes. Metal cations are complexed with the host molecules containing donor atoms or groups, such as dicyclohexano[18]-crown-6-ether and [2.2.2]cryptand, $\text{N}(\text{CH}_2\text{CH}_2\text{OCH}_2\text{CH}_2\text{OCH}_2\text{CH}_2)_3\text{N}$.^{6,7} Inclusion of various metal ions and alkylammonium was achieved by artificial design of the host molecules.⁸ Halonium⁹ is proposed as the intermediate of halogen addition reaction to alkene¹⁰ and halolactamization¹¹ and contributes as a component of square-shaped dinuclear Pt complexes.¹² Its isolation with the aid of inclusion using cyclic host molecules has attracted much less attention than inclusion of the metal cations. Resnati reported halogen bonding in which donor atoms have a significant interaction with halogen atoms of the compound and recognition of guests based on it.¹³ Recently, fluoronium “ F^+ ” sources, such as *Selectfluor* (a derivative from DABCO), *N*-fluorobenzenesulfonimide (NFSI) and *N*-fluoro-2,4,6-trimethylpyridinium hexafluorophosphate, have gathered attention as electrophiles in the electrophilic fluorination of arenes catalyzed by Pd and Cu.^{14,15} 1,2-Bis(2-pyridylethynyl)benzene (Scheme 1, bpeb), having two pyridyl groups tethered by a 1,2-dialkynyl benzene, functions as a *trans* bidentate ligand of transition metal complexes^{16,17} and the complexes of bromonium ions.^{18,19}



Scheme 1 Structure of bpeb, cpeb and Yoshida's macrocycle.

In this paper, we designed a cyclic organic host molecule composed of two pyridyl and two 1,2-dialkyl benzene units (cpeb) which is expected to have a similar N...N distance and a rigid structure, suited for complexation with haloniums. Here we report unique inclusion behavior of cpeb for the haloniums.

Results and discussion

Eqn (1) depicts the synthesis of cyclic pyridylethynylbenzene (cpeb) by deprotection of the $-\text{SiMe}_2\{(\text{CH}_2)_3\text{CN}\}$ group of **1** under basic conditions followed by the intramolecular Sonogashira–Hagihara cross-coupling reaction. The palladium(II) complex, $\text{Pd}(\text{OCOCF}_3)_2(\text{cpeb})$, was obtained by reaction of $\text{Pd}(\text{OCOCF}_3)_2$ and cpeb in 70% yield. Fig. 1 shows molecular structures of cpeb and its complex with the $\text{Pd}(\text{OCOCF}_3)_2$ guest determined by X-ray crystallography. Cpeb has a crystal polymorph (orthorhombic, *Cmce* (no. 64) and *Pbca* (no. 61)) depending on the recrystallization conditions (Fig. 1a and b). The crystal structure analyzed as *Cmce* (no. 64) has a 4-fold symmetry axis in which all the atoms are located within a single plane (Fig. 1a) while the two pyridine rings in the structure analyzed as *Pbca* (no. 61) are parallel in the molecule with a 2-fold axis (Fig. 1b). The molecular structure of $\text{Pd}(\text{OCOCF}_3)_2(\text{cpeb})$ adopts a square planar molecular

Chemical Resources Laboratory, Tokyo Institute of Technology, 4259 Nagatsuta, Midoriku, Yokohama 226-8503, Japan. E-mail: kosakada@res.titech.ac.jp; Fax: +81-45-924-5224

† Electronic supplementary information (ESI) available: Additional figures, UV and NMR spectra as well as theoretical calculation. CCDC 973075, 973076 and 973077. For ESI and crystallographic data in CIF or other electronic format see DOI: 10.1039/c3dt53629g

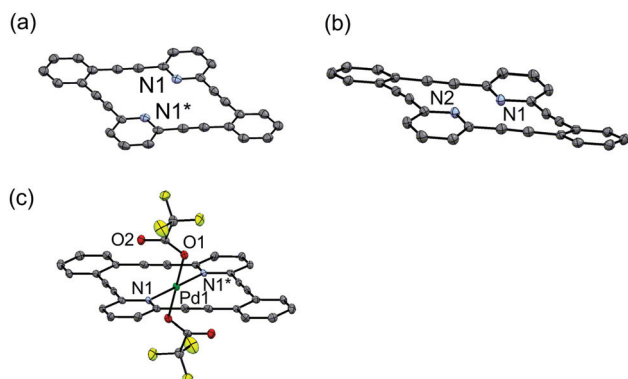
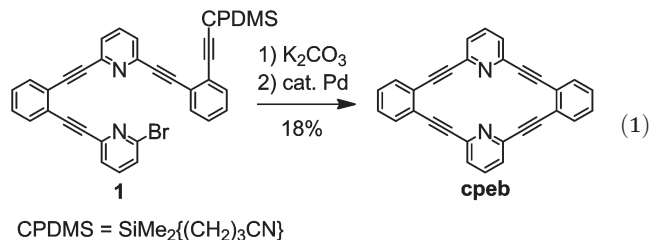


Fig. 1 Crystal structure of (a) cpeb (space group = *Cmce* (no. 64)), (b) cpeb (space group = *Pbca* (no. 61)) and (c) $\text{Pd}(\text{OCOCF}_3)_2(\text{cpeb})$.

geometry where pyridine units are located at *trans* positions to $\text{Pd}(\text{II})$. The Pd atom is located at the mid-point of the two nitrogen atoms of cpeb is 4.30 Å in both the structures (N1–N1* in Fig. 1a and N1–N2 in Fig. 1b). Yoshida *et al.* selected a macrocyclic molecule, a cyclyne-type azamacrocycle having two pyridine units and two 1,3-dialkyl benzenes as the host and found its light-emitting inclusion complex with $\text{Sb}(\text{V})\text{Cl}_5$.²⁰ Cpeb is estimated to have much shorter N–N distance and smaller binding space than the *meta*-substituted cyclic host. The N1–N1* distance of $\text{Pd}(\text{OCOCF}_3)_2(\text{cpeb})$ (4.09 Å) is shorter than the corresponding distance of cpeb, which is attributed to coordination of the $\text{Pd}(\text{II})$ ion.²¹

UV-vis spectroscopy measurements revealed a remarkable bathochromic shift of cpeb ($\lambda_{\text{max}} = 319$ nm) upon addition of Cl^+OTf^- ($\lambda_{\text{max}} = 357$ nm) and Br^+OTf^- ($\lambda_{\text{max}} = 358$ nm) (Fig. 2a, Table 1). The shoulder peaks are observed at *ca.* 400 nm in the spectra of the mixture of cpeb and X^+OTf^- (X = Cl, Br). Negligible change was observed in the reaction of cpeb and I^+OTf^- . The Job's plots of the absorption intensity at 410 nm of the mixture of cpeb and Br^+OTf^- ($[\text{cpeb}] + [\text{Br}^+\text{OTf}^-] = 1.0 \times 10^{-2}$ mM, CH_2Cl_2 , 25 °C) shows a maximum at a molar fraction close to 0.5, which indicates that cpeb and Br^+OTf^- form a 1 : 1 complex in CH_2Cl_2 solution.

Emission spectra also show the bathochromic shifts upon complexation of Cl^+ and Br^+ . Excitation of the mixture of cpeb and Cl^+OTf^- at $\lambda_{\text{ex}} = 357$ nm results in green emission ($\lambda_{\text{max}} = 508$ nm) with a Stokes shift of 1.00 eV and a moderate quantum yield ($\phi = 0.12$), while cpeb shows emission at $\lambda_{\text{max}} = 403$ nm with a smaller Stokes shift (0.81 eV) (Fig. 2b). The

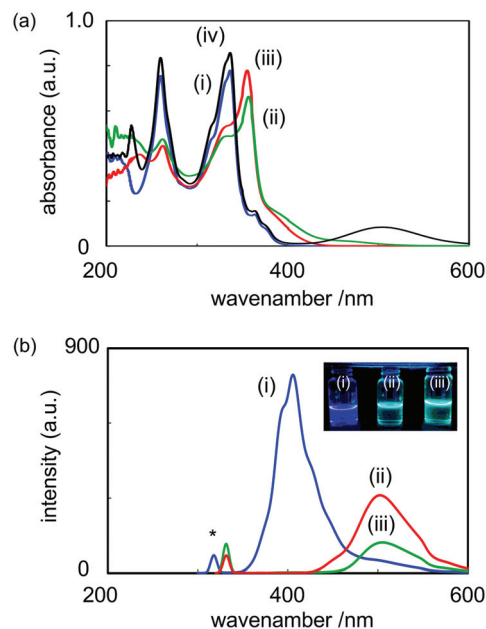


Fig. 2 (a) Absorption spectra of (i) cpeb (blue, $[\text{cpeb}] = 1.0 \times 10^{-2}$ mM), (ii) cpeb + Cl^+OTf^- (red, $[\text{Cl}^+\text{OTf}^-] = 1.0 \times 10^{-2}$ mM), (iii) cpeb + Br^+OTf^- (green, $[\text{Br}^+\text{OTf}^-] = 1.0 \times 10^{-1}$ mM) and (iv) cpeb + I^+OTf^- (black, $[\text{I}^+\text{OTf}^-] = 1.0 \times 10^{-1}$ mM) and (b) emission spectra of (i) cpeb (blue, $[\text{cpeb}] = 1.0 \times 10^{-3}$ mM), (ii) cpeb + Cl^+OTf^- (red, $[\text{Cl}^+\text{OTf}^-] = 1.0 \times 10^{-3}$ mM), and (iii) cpeb + Br^+OTf^- (green, $[\text{Br}^+\text{OTf}^-] = 1.0 \times 10^{-3}$ mM). Photograph under irradiation at 365 nm is shown in the inset ((i) cpeb, (ii) cpeb + Cl^+OTf^- , (iii) cpeb + Br^+OTf^-).

quantum yield from $\text{Cl}^+(\text{cpeb})$ ($\phi = 0.12$) is higher than that from $\text{Br}^+(\text{cpeb})$ ($\phi = 0.05$). The color change in light-emission before and after addition of X^+OTf^- (X = Cl, Br) to the solution of cpeb is clear (Fig. 2b, inset, $\lambda_{\text{ex}} = 365$ nm). The lifetime of emission from the mixture of cpeb and Br^+OTf^- ($\tau_0 = 10$ ns) is longer than that from cpeb ($\tau_0 = 6.5$ ns). The solid-state emission from cpeb ($\lambda_{\text{max}} = 406$ nm, $\phi = 0.14$ (absolute)) is similar to that from the solution while the solid obtained by the evaporation of the mixture of cpeb and X^+OTf^- (X = Cl, Br) is not emissive ($\phi < 0.01$ (absolute)).

HR-ESI-MS spectra of the mixture of cpeb and Br^+OTf^- in CH_2Cl_2 showed mass peaks assigned to $\text{Br}(\text{cpeb})$ ($m/z = 483.029$, calcd 483.032). HR-ESI-MS spectra of the mixture of cpeb and Cl^+OTf^- showed mass peaks at $m/z = 509.0306$ and 913.1532 which are assigned to the hydrochloric acid adducts of the complex, $\text{Cl}(\text{cpeb})(\text{HCl})_2$ (calcd 509.0346) and $\text{Cl}_3(\text{cpeb})_2(\text{HCl})_2$ (calcd 913.1505), respectively. ^1H NMR spectra of the mixture of cpeb and X^+OTf^- (X = Cl, Br) in CD_2Cl_2 showed a broad signal at δ 7.5–8.0 while free cpeb showed clearly separated signals (δ 7.63 ($\text{C}_5\text{H}_3\text{N}$), 7.59 (C_6H_4), 7.44 ($\text{C}_5\text{H}_3\text{N}$), 7.34 (C_6H_4)). It suggests equilibration of the complex formation of cpeb and X^+OTf^- (X = Cl, Br) on the NMR time scale.

Similar complexation and bathochromic shifts are observed for the mixture of cpeb with AgOTf , $\text{Pd}(\text{OCOCF}_3)_2$, $\text{Zn}(\text{OTf})_2$ and CF_3COOH (Table 1). The reaction of cpeb with $\text{Pd}(\text{OCOCF}_3)_2$ causes quenching of fluorescence in solution

Table 1 Photochemical data of compounds

Compound	Absorption ^a $\lambda_{\text{max}}/\text{nm}$	Emission ^b			Stokes shift ^d /eV (nm ⁻¹)
		$\lambda_{\text{max}}/\text{nm}$	ϕ^c	τ_0/ns	
cpeb	319	403 (406) ^e	0.15 (0.14) ^e	6.5	0.81 (84)
cpeb + Cl ⁺ ^k	357	508 (—) ^e	0.12 (<0.01) ^e	—	1.00 (169)
cpeb + Br ⁺ ^j	358	503 (—) ^e	0.05 (<0.01) ^e	10	0.99 (171)
cpeb + Ag ⁺ ^f	332	501	0.03	—	1.25 (169)
cpeb + Pd ²⁺ ^g	330	—	—	—	—
cpeb + Zn ²⁺ ^h	332	504 (485) ^e	0.09 (0.15) ^e	5.7	1.27 (172)
cpeb + H ⁺ ⁱ	353	495 (495) ^e	0.16 (0.19) ^e	9.7	1.00 (113)

^a [cpeb] = 1.0×10^{-2} mM, CH₂Cl₂, 25 °C. ^b [cpeb] = 1.0×10^{-3} mM, CH₂Cl₂, 25 °C, $\lambda_{\text{ex}} = \lambda_{\text{max}}(\text{absorption})$. ^c Quantum yield. ^d Stokes shift, $\Delta\lambda = \lambda_{\text{max}}(\text{absorption}) - \lambda_{\text{max}}(\text{emission})$. ^e Data in solid state. ^f AgOTf (2 equiv. to cpeb). ^g Pd(OCOCF₃)₂ (4 equiv. to cpeb). ^h Zn(OTf)₂ (2 equiv. to cpeb). ⁱ CF₃COOH (1.0 mM). ^j Br⁺OTf⁻ (1 equiv. to cpeb). ^k Cl⁺OTf⁻ (1 equiv. to cpeb).

probably due to a heavy atom effect. The mixture of cpeb and Zn(OTf)₂ has similar emission both from the solution and from the solid state (in solution, $\lambda_{\text{max}} = 504$ nm, $\phi = 0.09$; in solid state, $\lambda_{\text{max}} = 485$ nm, $\phi = 0.15$ (absolute)). The complexation of CF₃COOH and cpeb requires a large excess of CF₃COOH ([cpeb] = 1.0×10^{-3} mM, [CF₃COOH] = 1.0×10^{-1} mM) to reach a saturation point in emission, which indicates a relatively lower ability of cpeb for complexation with H⁺ than other cations described above. The complex of cpeb and CF₃COOH shows also emission both from the solution and from the solid state (in solution, $\lambda_{\text{max}} = 495$ nm, $\phi = 0.16$; in solid state, $\lambda_{\text{max}} = 495$ nm, $\phi = 0.19$ (absolute)).

Fig. 3 illustrates the structure of a rhomboid-shaped cyclic pyridylethynyl benzene (cpeb) employed in this study and its plausible structures in the inclusion complexes. The smaller guest, such as Cl⁺ and H⁺, may form an unsymmetric inclusion complex g(cpeb) in which the guest prefers unsymmetrical coordination with one donor atom. The guest molecule, such as Br⁺, Ag⁺, Pd²⁺ and Zn²⁺, whose size is similar to the cavity of the cpeb may form a symmetric inclusion complex G(cpeb) (G = guest) in which the guest molecule (or ion) is located at the midpoint of the nitrogen atom. A larger size ion such as I⁺ may not be included due to the shape-persistence of cpeb.

Fig. 4 shows the calculated energy potentials for the position of halonium in an N-X⁺-N system in X(cpeb) (X = Cl⁺, Br⁺) using the ORCA package (version 2.9.1).²² The diagram of

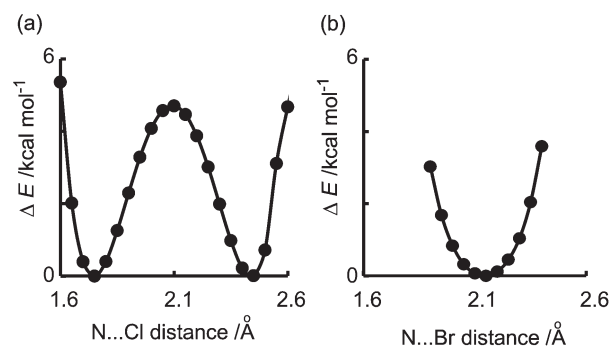


Fig. 4 Calculated potential energy curve and the N(1)...X distance in N(1)...X...N(2) in (a) [Cl⁺(cpeb)] and (b) [Br⁺(cpeb)]. The energies for the model structures of (X)(cpeb) were calculated at every 0.05 Å distance of the rigid N(1)...X...N(2) unit (N(1)...N(2) = 4.19 Å) using the PBE38/TZVP basis set.²³

Cl(cpeb) and Br(cpeb) was calculated to have a double-well and single-well potential system, respectively. The results indicate that Cl⁺ in an N-X⁺-N system of Cl⁺(cpeb) prefers the position close to one nitrogen than the other. Br⁺ in the Br(cpeb) system is located at the midpoint of N-X⁺-N with similar interactions of Br⁺ and the two nitrogen atoms. Erdélyi investigated the complexation of halonium and deuterated bis(2-pyridylethynyl)benzene by NMR spectroscopy as well as DFT calculation in which the bromonium cation is included at the midpoint of the nitrogen atoms of two pyridyl groups.¹⁹ The optimization calculation for I⁺(cpeb) did not converge well due to the instability of the complex.²⁴

These results can be rationalized by the fitting of the halonium ions and the cavity of cpeb. The N1-N1* distance in cpeb analyzed by X-ray crystallography is 4.30 Å which is shorter than the corresponding N...N distance in bis(2,6-dimethylpyridyl)iodonium dibromiodate, [I(C₅H₃N-2,6-Me₂)₂]⁺[BrIBr]⁻ (N...N = 4.588 Å),²⁵ and slightly longer than that in bis(quinoline)bromine perchlorate, [Br(quinoline)₂]ClO₄, (N...N = 4.285 Å),^{26,27} indicating that the N...N distance in cpeb is not long enough for inclusion of I⁺ and appropriate for Br⁺ inclusion. A relatively smaller Cl⁺ tends to coordinate strongly to one nitrogen to form an unsymmetric inclusion structure. Similar analysis by calculation for the complex

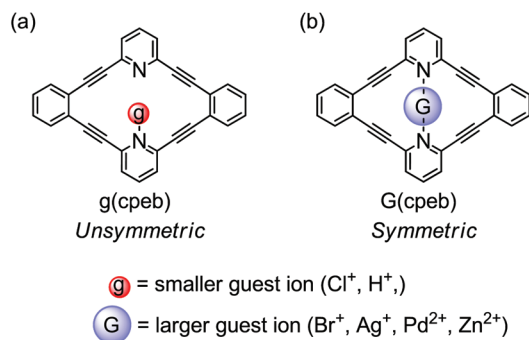


Fig. 3 Structure of the inclusion complex of cpeb with (a) smaller (Cl⁺, H⁺) and (b) larger (Br⁺, Ag⁺, Pd²⁺, Zn²⁺) guest ions.

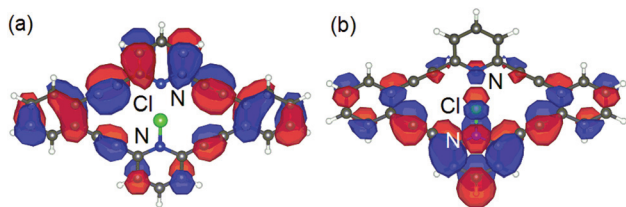


Fig. 5 The (a) HOMO and (b) LUMO of the ground state of Cl(cpeb) calculated by DFT calculation (PBE38/TZVP).

X(cpeb) (X = H, Zn, Ag) suggests a symmetric structure for large guest ions (Zn, Ag) and an unsymmetric structure for a relatively smaller ion (H) which is also explained by the size of the guest ions.

Fig. 5 shows the calculated HOMO and LUMO of the ground state of Cl⁺(cpeb) which has an unsymmetric ground state with a short distance between the Cl⁺ and one nitrogen, as described above; LUMO orbital is localized from Cl⁺ to phenylene units. Br(cpeb) was calculated to have a symmetric ground state structure which has LUMO spread over the cpeb molecule.

Since the emission from a symmetric structure (LUMO to HOMO) is derived from a forbidden transition,²⁸ the observed emission from Br⁺(cpeb) probably involves formation of an unsymmetric transition state generated by intramolecular relaxation after excitation. The lower quantum yield of emission from Br⁺(cpeb) ($\phi = 0.05$) than that from Cl⁺(cpeb) ($\phi = 0.12$) and relatively longer lifetime of emission from Br(cpeb) ($\tau_0 = 10$ ns) are ascribed to the large structural change from the symmetric ground state structure of Br(cpeb) to the transition state with an unsymmetric structure. The absorption shoulder peak at 400 nm observed in the mixture of cpeb and Cl⁺OtF is assigned to charge transfer (CT)-type absorption by TD-DFT (PBE38/TZVP) calculation suggesting that the emission of X⁺(cpeb) (calculated to be 504 nm with oscillator strength $f = 0.04$ (for Cl) and 457 nm with $f = 0.03$ (for Br)) mainly consists of a transition from HOMO to LUMO. TD-DFT (PBE38/TZVP) calculation suggests that the absorption peaks of cpeb observed at 259, 318 and 340 nm mainly consist of a transition from HOMO–1 to LUMO (calcd 285.9 nm), HOMO to LUMO (calcd 304.8 nm), and HOMO to LUMO+1 (calcd 340.4 nm, forbidden transition) respectively.

Conclusion

We synthesized a facile shape-persistent azamacrocyclic molecule, cpeb, having two pyridyl units and observed its size selective inclusion of halonium ions, Cl⁺, Br⁺ and I⁺. Cl⁺ and Br⁺ form unsymmetric and symmetric inclusion complexes, respectively, while I⁺ does not form an inclusion complex. The different types of inclusion of cpeb for halonium as well as Ag, Pd, Zn and H are ascribed to the matching and mismatching of the size of guest ions and the cavity of cpeb.

Experimental

General

1,2-Diethynylbenzene²⁹ was prepared by literature methods. Other chemicals were commercially available. ¹H and ¹³C{¹H} NMR spectra were acquired on a Varian MERCURY-300 (300 MHz) and a Bruker AV-400M (400 MHz). Fast atom bombardment mass spectra (FABMS) and HR-ESI-TOF-MS were obtained on a JEOL JMS-700 (matrix, 2-nitrophenyl *n*-octyl ether (NPOE)) and a microTOF II (Bruker) spectrometer respectively. Elemental analyses were carried out with a Yanaco MT-5 CHN autorecorder. UV-visible absorption spectra were measured on a JASCO V-530 for 1.0×10^{-2} mM solutions in CH₂Cl₂. Photoluminescence spectra were recorded for 1.0×10^{-3} M solutions in CH₂Cl₂. Quantum yields were estimated by comparison of the standard solution of quinine sulfate (1.0 M, $\phi = 0.546$). The lifetime of the emission from the compounds was measured using the Time-Resolved Absorption and emission Spectra Analysis System (TRASAS) in our institute equipped with an Nd-YAG laser ($\lambda_{\text{ex}} = 355$ nm, [compound] = 0.00001 mM, in CH₂Cl₂). Solid state photoluminescence spectra were recorded using an absolute PL quantum yield measurement system (C9920-01, Hamamatsu Photonics K. K.) equipped with a Xe light source, a monochromator, an integrating sphere, and a CCD spectrometer.

Synthesis of 1,2-bis(6-bromo-2-ethynylpyridyl)benzene (2)

A THF solution (300 mL) of 2,6-dibromopyridine (19.0 g, 80 mmol) and Et₃N (27.8 mL, 200 mmol) was degassed by freeze–pump–thaw cycles. To the solution, CuI (190 mg, 1.0 mmol), PdCl₂(PPh₃)₂ (702 mg, 1.0 mmol) and 1,2-diethynylbenzene (2.52 g, 20 mmol) were successively added and then the mixture was stirred for 48 h at 50 °C. After removal of the solvent by evaporation, the organic products were dissolved in CH₂Cl₂ (300 mL), and the solution was washed with sat. NH₄Cl(aq) (100 mL). The separated organic phase was dried over MgSO₄, filtered and evaporated to form a crude product as a yellow oil. Purification by silica gel column chromatography (eluent: CH₂Cl₂–hexane = 2/1, $R_f = 0.65$) yielded 1,2-bis(6-bromo-2-ethynylpyridyl)benzene (2) (4.01 g, 9.15 mmol, 46%) as a yellow powder. Anal. Calcd for C₂₀H₁₀Br₂N₂, C: 54.83, H: 2.30, N: 6.39%. Found, C: 54.99, H: 2.22, N: 6.26%. ¹H NMR (300 MHz, CDCl₃, r.t.) δ 7.85 (d, 2H, 3-C₅H₄N, $J = 8$ Hz), 7.64 (dd, 2H, *m*-C₆H₄, $J = 6, 3$ Hz), 7.63 (t, 2H, 4-C₅H₄N, $J = 8$ Hz), 7.47 (d, 2H, 5-C₅H₄N, $J = 8$ Hz), 7.40 (dd, 2H, *o*-C₆H₄, $J = 6, 3$ Hz). ¹³C{¹H} NMR (100 MHz, CDCl₃, r.t.) δ 144.0, 141.8, 138.7, 132.3, 129.3, 127.7, 127.0, 125.6, 92.3 (C≡C), 89.2 (C≡C). HRMS (ESI-TOF-MS): calcd for C₂₀H₁₁Br₂N₂ 438.9383; found, m/z 438.9253 [M + H]⁺.

Synthesis of C₆H₄-1,2-(C≡C-H)(C≡C-CPDMS)

A THF–MeOH (100 mL/100 mL) solution containing C₆H₄-1,2-(C≡C–TMS)₂ (2.71 g, 10 mmol) and K₂CO₃ (6.9 g, 50 mmol) was stirred at room temperature for 12 h. The separated organic phase was dried over MgSO₄ and evaporated to yield C₆H₄-1,2-(C≡C–H)₂ which was dissolved in dry THF (80 mL).

To the solution, EtMgBr (1 M solution in THF, 10 mL, 10 mmol) was added at 0 °C, and then the mixture was stirred for 3 h. To the resulting solution ClSiMe₂{(CH₂)₃CN} (1.49 g, 11 mmol) was added at room temperature, and then the mixture was stirred for 24 h. The product was extracted with CH₂Cl₂ and washed with water. The separated organic phase was dried over MgSO₄, filtered and evaporated to form a crude product as a yellow oil. Purification by silica gel column chromatography (eluent: CH₂Cl₂–hexane = 1/1, *R_f* = 0.4) yielded C₆H₄-1,2-(C≡C–H)(C≡C–CPDMS) (2.31 g, 8.7 mmol, 87%) as a colorless oil. ¹H NMR (300 MHz, CDCl₃, r.t.) δ 7.51–7.45 (m, 2H), 7.32–7.27 (m, 2H), 3.33 (s, 1H, ≡C–H), 2.44 (t, 2H, CH₂CN, *J* = 6.8 Hz), 0.86 (m, 2H, CH₂), 0.27 (s, 6H, Me).

Synthesis of 1-(6-[(3'-cyanopropyl)dimethylsilyl]acetyl)-2-ethynylpyridyl)-2-(6-bromo-2-ethynylpyridyl)benzene (1)

A THF solution (20 mL) of **2** (1.75 g, 4.0 mmol) and Et₃N (40 mL, 290 mmol) was degassed by freeze–pump–thaw cycles. To the solution, CuI (38 mg, 0.20 mmol), PdCl₂(PPh₃)₂ (140 mg, 0.20 mmol) and C₆H₄-1,2-(C≡C–H)(C≡C–CPDMS) (1.06 g, 4.0 mmol) were successively added, and then the mixture was stirred for 36 h at 50 °C. The resulting mixture was concentrated by evaporation. The obtained organic product was dissolved in CH₂Cl₂ (300 mL) and the solution was washed with sat. NH₄Cl(aq) (100 mL). The separated organic phase was dried over MgSO₄, filtered and evaporated to form a crude product as a yellow oil. Purification by silica gel column chromatography (eluent: CH₂Cl₂–hexane = 2/1, *R_f* = 0.40) yielded **1** (834 mg, 1.37 mmol, 34%) as a brown solid. ¹H NMR (300 MHz, CDCl₃, r.t.) δ 7.91 (d, 1H, C₅H₄N, *J* = 8 Hz), 7.85 (d, 1H, C₅H₄N, *J* = 8 Hz), 7.79 (t, 1H, *p*-C₅H₄N, *J* = 8 Hz), 7.63–7.66 (m, 2H, C₆H₄), 7.58 (dd, 1H, C₆H₄, *J* = 6, 3 Hz), 7.54 (t, 1H, *p*-C₅H₄N, *J* = 8 Hz), 7.49–7.53 (m, 2H, C₆H₄, C₅H₄N), 7.37–7.41 (m, 3H, C₆H₄, C₅H₄N), 7.34 (dd, 2H, C₆H₄, *J* = 6, 3 Hz), 2.34 (t, 2H, CH₂, *J* = 7 Hz), 1.73–1.83 (m, 2H, CH₂, C₅H₄N), 0.80 (m, 2H, CH₂), 0.23 (s, 6H, Me). ¹³C{¹H} NMR (100 MHz, CDCl₃, r.t.) δ 144.0, 143.9, 143.7, 141.8, 138.8, 136.8, 132.6, 132.5, 132.2, 132.2, 129.3, 129.1, 129.0, 128.7, 127.7, 127.4, 127.2, 126.7, 125.9, 125.8, 125.5, 125.1, 119.9 (CN), 104.5 (C≡C), 97.4 (C≡C), 93.1 (C≡C), 92.3 (C≡C), 92.2 (C≡C), 89.3 (C≡C), 88.1 (C≡C), 88.0 (C≡C), 20.8 (CH₂), 20.6 (CH₂), 15.7 (CH₂), –1.7 (Me). Anal. Calcd for C₃₆H₂₆BrN₃Si, C: 71.05, H: 4.31, Br: 13.13, N: 6.90%. Found, C: 70.33, H: 4.24, Br: 12.71, N: 6.60%. HRMS (ESI-TOF-MS): calcd for C₃₆H₂₆BrN₃Si + Na: 630.0977, found: *m/z* = 630.0970 [*M* + Na⁺].

Synthesis of cpeb

A THF–MeOH solution (THF–MeOH = 50 mL/50 mL) containing **1** (609 mg, 1.0 mmol) and K₂CO₃ (690 mg, 5.0 mmol) was stirred at room temperature for 12 h. After removal of the solvent by evaporation, the obtained organic product was dissolved in CH₂Cl₂ (300 mL) and the solution was washed with water (50 mL). The separated organic phase was dried over MgSO₄, filtered and evaporated to yield C₆H₄-1-(C≡C–C₆H₃N-6-C≡C–C₆H₄-2-C≡CH)-2-(C≡C–C₆H₃N–Br) as a yellow oil. The above product was dissolved in THF–Et₃N (100 mL/

100 mL), and the solution was degassed by freeze–pump–thaw cycles. To the mixture, CuI (9.5 mg, 0.05 mmol) and PdCl₂(PPh₃)₂ (35 mg, 0.005 mmol) were successively added, and the solution was stirred at 50 °C for 48 h. The resulting mixture was concentrated by evaporation. The obtained organic product was dissolved in CH₂Cl₂ (200 mL) and the solution was washed with sat. NH₄Cl(aq) (100 mL). The separated organic phase was dried over MgSO₄, filtered and evaporated to yield a crude product as a black solid. Purification by silica gel column chromatography (eluent: CH₂Cl₂–hexane = 2/1, *R_f* = 0.40) yielded cpeb (834 mg, 1.37 mmol, 34%) as a brown powder. ¹H NMR (400 MHz, CD₂Cl₂, r.t.) δ 7.34 (dd, 4H, *o*-C₆H₄, *J* = 6, 3 Hz), 7.44 (d, 4H, 3-C₅H₄N, *J* = 8 Hz), 7.59 (dd, 4H, *m*-C₆H₄, *J* = 6, 3 Hz), 7.63 (t, 2H, 4-C₅H₄N, *J* = 8 Hz). ¹³C{¹H} NMR (100 MHz, CD₂Cl₂, r.t.) δ 144.3 (2-C₅H₄N), 136.8 (4-C₅H₄N), 133.1 (*o*-C₆H₄), 129.5 (*m*-C₆H₄), 126.9 (3-C₅H₄N), 125.9 (*ipso*-C₆H₄), 93.3 (C≡C), 87.6 (C≡C). HRMS (ESI-TOF-MS): calcd for C₃₀H₁₄N₂ + Na: 425.1055, found: *m/z* = 425.1049 [*M* + Na⁺].

Synthesis of Pd(OCOCF₃)₂(cpeb)

A CH₂Cl₂ solution of cpeb (50 mM, 10 mL, 5 μmol) was added to the THF solution of CF₃COOH (5.0 mM, 1.2 mL, 6.0 μmol), and the mixture was stirred at 50 °C for 12 h. The separated brown solid of Pd(OCOCF₃)₂(cpeb) was collected by filtration (2.6 mg, 3.5 μmol, 70%). HRMS (ESI-TOF-MS): calcd for C₃₀H₁₄N₂Pd: 508.0182, found: *m/z* = 508.0213 [*M*-2(OCOCF₃)₂]⁺. Low solubility of the compound prevented NMR measurements. A similar reaction in CDCl₃ without stirring yielded Pd(OCOCF₃)₂(cpeb) as single crystals which were subjected to X-ray structure analyses.

X-ray structure analyses

Crystals of cpeb and Pd(OCOCF₃)₂(cpeb) suitable for X-ray diffraction study were obtained by recrystallization from CH₂Cl₂ (cpeb (*Cmce* (no. 64)), CH₂Cl₂/HCl(aq) (cpeb (*Pbca* (no. 61)) and CDCl₃ (Pd(OCOCF₃)₂(cpeb)). All measurements were made on a Rigaku AFC-10R Saturn or Bruker ApexII CCD diffractometer with graphite monochromated Mo-Kα radiation. Calculations were carried out using a program package Crystal Structure™ for Windows.³⁰ All hydrogen atoms were included at the calculated positions with fixed thermal parameters.

Acknowledgements

We thank our colleagues in the Chemical Resources Laboratory of the Tokyo Institute of Technology for their technical support and discussions, Dr Yoshihisa Sei for X-ray crystallography and life-time measurements in the Center for Advanced Materials Analysis of our institute, and Dr Takanori Fukushima and Dr Yoshiaki Shoji for measurement of emission spectra (solid state). This work was supported by a Grant-Aid for Scientific Research for Young Scientists from the Ministry of Education, Culture, Sports, Science and Technology, Japan

(25810059), and for Scientific Research on Innovative Areas "Coordination Program" (24108711).

Notes and references

- 1 R. M. Izatt, K. Pawlak and J. S. Bradshaw, *Chem. Rev.*, 1991, **91**, 1721.
- 2 (a) C. H. Park and H. E. Simmons, *J. Am. Chem. Soc.*, 1968, **90**, 2431; (b) B. Dietrich, J.-M. Lehn and J. P. Sauvage, *Tetrahedron Lett.*, 1969, **34**, 2885; (c) J. M. Llinares, D. Powell and K. Bowman-James, *Coord. Chem. Rev.*, 2003, **240**, 57; (d) V. Amendola, L. Fabbri, C. Mangano, P. Pallavicini, A. Poggi and A. Taglietti, *Coord. Chem. Rev.*, 2001, **219–221**, 821; (e) J. Nelson, V. McKee and G. Morgan, *Prog. Inorg. Chem.*, 1998, **47**, 167.
- 3 (a) C. D. Gutsche, B. Dhawan, K. H. No and R. Muthukrishnan, *J. Am. Chem. Soc.*, 1981, **103**, 3782; (b) C. D. Gutsche, in *Calixarenes*, The Royal Society of Chemistry, Cambridge, 1989; (c) *Calixarenes: A Versatile Class of Macrocyclic Compounds*, ed. J. Vicens and V. Böhmer, Kluwer Academic Publishers, Dordrecht, 1991; (d) V. Böhmer, *Angew. Chem., Int. Ed. Engl.*, 1995, **34**, 713.
- 4 (a) T. Ogoshi, S. Kanai, S. Fujinami, T. Yamagishi and Y. Nakamoto, *J. Am. Chem. Soc.*, 2008, **130**, 5022; (b) T. Ogoshi, Y. Nishida, T. Yamagishi and Y. Nakamoto, *Macromolecules*, 2010, **43**, 3145; (c) T. Ogoshi, K. Kitajima, T. Aoki, S. Fujinami, T. Yamagishi and Y. Nakamoto, *J. Org. Chem.*, 2010, **75**, 3268.
- 5 (a) K. Harata, *Chem. Rev.*, 1998, **98**, 1803; (b) H.-J. Schneider, F. Hacket and V. Rüdiger, *Chem. Rev.*, 1998, **98**, 1755; (c) W. Saenger, J. Jacob, K. Gessler, T. Steiner, D. Hoffmann, H. Sanbe, K. Koizumi, S. M. Smith and T. Takaha, *Chem. Rev.*, 1998, **98**, 1787.
- 6 I.-H. Chu, H. Zhang and D. V. Dearden, *J. Am. Chem. Soc.*, 1993, **115**, 5736.
- 7 J. M. Lehn and J. P. Sauvage, *J. Am. Chem. Soc.*, 1975, **97**, 6700.
- 8 K. Bowman-James, *Acc. Chem. Res.*, 2005, **38**, 671.
- 9 (a) G. A. Olah, *Halonium Ions*, Wiley, New York, 1975; (b) V. V. Grushin, *Chem. Soc. Rev.*, 2000, **29**, 315; (c) R. S. Brown, R. W. Nagorski, A. J. Bennet, R. E. D. McClung, G. H. M. Aarts, M. Klobukowski, R. McDonald and B. D. Santarsiero, *J. Am. Chem. Soc.*, 1994, **116**, 2448.
- 10 I. Roberts and G. E. Kimball, *J. Am. Chem. Soc.*, 1937, **59**, 947.
- 11 (a) R. B. Grossman and R. J. Trupp, *Can. J. Chem.*, 1998, **76**, 1233; (b) X.-L. Cui and R. S. Brown, *J. Org. Chem.*, 2000, **65**, 5653; (c) R. S. Brown, A. A. Neverov, C. T. Liu and C. I. Maxwell, in *In Recent Developments in Carbocation and Onium Ion Chemistry*, ed. K. Laali, American Chemical Society, Washington, 2007, 458; (d) J. Haas, S. Piguel and T. Wirth, *Org. Lett.*, 2002, **4**, 297; (e) J. Haas, S. Bissmire and T. Wirth, *Chem.-Eur. J.*, 2005, **11**, 5777.
- 12 (a) P. J. Stang and V. V. Zhdankin, *J. Am. Chem. Soc.*, 1993, **115**, 9808; (b) P. J. Stang and K. Chen, *J. Am. Chem. Soc.*, 1995, **117**, 1667.
- 13 (a) P. Metrangolo, H. Neukirch, T. Pilati and G. Resnati, *Acc. Chem. Res.*, 2005, **38**, 386; (b) J. Lin, J. Martí-Rujas, P. Metrangolo, T. Pilati, S. Radice, G. Resnati and G. Terraneo, *Cryst. Growth Des.*, 2012, **12**, 5757.
- 14 (a) K. L. Hull, W. Q. Anani and M. S. Sanford, *J. Am. Chem. Soc.*, 2006, **128**, 7134; (b) N. D. Ball and M. S. Sanford, *J. Am. Chem. Soc.*, 2009, **131**, 3796; (c) T. Furuya, H. M. Kaiser and T. Ritter, *Angew. Chem., Int. Ed.*, 2008, **47**, 5993; (d) T. Furuya and T. Ritter, *J. Am. Chem. Soc.*, 2008, **130**, 10060; (e) T. Furuya, A. E. Strom and T. Ritter, *J. Am. Chem. Soc.*, 2009, **131**, 1662; (f) A. W. Kaspi, A. Yahav-Levi, I. Goldberg and A. Vigalok, *Inorg. Chem.*, 2008, **47**, 5; (g) D. C. Powers and T. Ritter, *Nat. Chem.*, 2009, **1**, 302; (h) P. S. Fier, J. Luo and J. F. Hartwig, *J. Am. Chem. Soc.*, 2013, **135**, 2552.
- 15 M. D. Struble, M. T. Scerba, M. Siegler and T. Lectka, *Science*, 2013, **340**, 57.
- 16 E. Bosch and C. L. Barnes, *Inorg. Chem.*, 2001, **40**, 3097.
- 17 Y. Suzaki, K. Shimada, E. Chihara, T. Saito, Y. Tsuchido and K. Osakada, *Org. Lett.*, 2011, **13**, 3774.
- 18 A. A. Neverov, H. X. Feng, K. Hamilton and R. S. Brown, *J. Org. Chem.*, 2003, **68**, 3802.
- 19 (a) A.-C. C. Carlsson, J. Gräfenstein, J. L. Laurila, J. Bergquist and M. Erdélyi, *Chem. Commun.*, 2012, **48**, 1458; (b) A.-C. C. Carlsson, J. Gräfenstein, A. Budnjo, J. L. Laurila, J. Bergquist, A. Karim, R. Kleinmaier, U. Brath and M. Erdélyi, *J. Am. Chem. Soc.*, 2013, **134**, 5706; (c) M. Erdélyi, *Chem. Soc. Rev.*, 2012, **41**, 3547.
- 20 S. Kobayashi, Y. Yamaguchi, T. Wakamiya, Y. Matsubara, K. Sugimoto and Z. Yoshida, *Tetrahedron Lett.*, 2003, **44**, 1469.
- 21 M. Jung, Y. Suzaki, T. Saito, K. Shimada and K. Osakada, *Polyhedron*, 2012, **40**, 168.
- 22 F. Neese, *WIREs Comput. Mol. Sci.*, 2012, **2**, 73.
- 23 G. J. Antony, S. Ehrlich and H. Krieg, *J. Chem. Phys.*, 2010, **132**, 154104.
- 24 Similar calculations were conducted by LPNO-CEPA/1, DFT(B3LYP, PBE38) and MP2. The result from PBE38 is similar to those from LPNO-CEPA/1 and LPNO-CCSD which are known as accurate theories of electron correlation. The results indicate that the result from PBE38 possesses higher reliability. B3LYP, employed in previous investigation for halonium–nitrogen coordination (ref. 19), estimate also double-well potential curve with the smaller energy barrier in which the local minima for N–Cl distances is shorter than those from LPNO-CEPA/1, LPNO-CCSD and PBE38. The result from MP2 calculation is different from those of the above methods, which has one local minimum.

- 25 A. S. Batsanov, A. P. Lightfoot, S. J. R. Twiddle and A. Whiting, *Acta Crystallogr., Sect. E: Struct. Rep. Online*, 2006, **62**, o901.
- 26 (a) A. S. Batsanov, J. A. K. Howard, A. P. Lightfoot, S. J. R. Twiddle and A. Whiting, *Eur. J. Org. Chem.*, 2005, 1876; (b) G. Brayer and M. N. G. James, *Acta Crystallogr., Sect. B: Struct. Crystallogr. Cryst. Chem.*, 1982, **38**, 654; (c) O. Hassel and H. Hope, *Acta Chem. Scand.*, 1961, **15**, 407; (d) C. Álvarez-Rúa, S. García-Granda, A. Ballesteros, F. González-Bobes and J. M. González, *Acta Crystallogr., Sect. E: Struct. Rep. Online*, 2002, **58**, o1381; (e) J. M. Chalker, A. L. Thompson and B. G. Davis, *Org. Synth.*, 2010, **87**, 288.
- 27 N. W. Alcock and G. B. Robertson, *J. Chem. Soc., Dalton Trans.*, 1975, 2483.
- 28 S1 state of the excited state of Br⁺(cpeb) is calculated to have a symmetric ground state structure.
- 29 C. Huynh and G. Linstrumelle, *Tetrahedron*, 1988, **44**, 6337.
- 30 *Crystal Structure: Crystal analysis package*, Rigaku and Rigaku/MS (2000–2014).